Robust Leader-Follower Formation Control for Human-Robot Scenarios

Alia Gilbert, Vishnu S. Chipade, Dimitra Panagou

***Abstract*— This paper studies a robust control design problem for multi-robot formation control around a human leader in the presence of measurement uncertainties. Utilizing previous work on adaptive estimation algorithms and Lyapunov-like barrier functions for collision avoidance and connectivity maintenance, an architecture is designed for leader-follower formation control for a multi-robot system to achieve a desired formation around a human leader while maintaining connectivity and avoiding collisions in the presence of uncertainties in the leader's and follower robots' own state information. Convergence and safety of the follower robots is proved formally. The proposed architecture is demonstrated in simulations as well as in experiments.**

I. Introduction

A. Motivation

Multi-agent systems has now become a diverse and popular field due to the value from real-world application as well as research areas. In many real-world applications, robots do not have perfect knowledge of their own state or of their sensing targets. Therefore considering uncertainty within the context of multi-agent task objectives and tracking is an important research topic. In addition, humans-robot collaboration is becoming more critical as robots enter manufacturing, construction, and maintenance domains, for example. In these real-life scenarios, robots will not have perfect knowledge of their own states, each other's states, or the human's state. Many existing algorithms, however, do not take into consideration uncertainty in both object tracking and self-states. In this paper, we study a problem of leader-follower formation control for a multi-robot system around a human leader in the presence of uncertainties in the robots' own states and the human's state.

B. Related Work

Formation control is a well studied research area [1] be it leader-follower based formation control [2] or artificial potential field-based formation [3] or consensus based approach [4] or neural network based approaches for formation control [5]. Several attempts have also been made to account for uncertainties in the formation control problems. For example, in [6] authors develop an adaptive leader-following consensus control for multi-agent systems under bounded process noise using model reference adaptive control approach, but do not provide experimental verification. A similar problem with process noise is also considered in [7] where an event triggered mechanism is proposed to achieve consensus. Authors in [8] design leader-follower control using potential function based high-gain feedback control when there is uncertainty in the leader's state, but do not make any guarantees on safety or have experimental data. Lyapunov-like barrier functions have been developed whose gradients are used for collision avoidance and connectivity maintenance in [9], in which no uncertainty in state measurements is considered. Collision avoidance and connectivity maintenance with uncertainty has been explored in [10], where the authors consider uncertain nonlinear dynamics with Model Predictive Controller (MPC) implementation, but the findings, again, did not have experimental results.

Leader-follower control is also applied to human-robot scenarios to guide robots formation, for example in [11] by using haptic feedback and in [12] by hand gestures, but do not consider safety in the controls of the robots. Human-robot interactions often require estimation of human's state exogenously as the human may not be actively communicating its state to the robots. In [13] authors develop an adaptive estimation algorithm to estimate states of human using external sensing inputs, which was verified only with simulation results.

C. Overview and Contributions

In this paper, we build on the coordination control protocol for multi-agent systems as designed in [9] to provide a robust leader-follower formation control that takes into account the uncertainties in the follower robots' own states and uncertainty in the leader's state, where the follower robots are trying to measure the leader's state exogenously. By exogenously here we mean that the leader is not necessarily communicating its state information to the follower robots but rather the follower robots are trying to measure the leader's state using their onboard sensors or some external sensors. For example when a human is the leader and robots are followers, the robots will have to estimate human's state using either their onboard sensors (for example, camera, lidar, etc,.) or some external sensors. We use the adaptive active-passive estimation algorithms [13] to estimate the leader's state and a Kalman filter to estimate robots' own

A. Gilbert is with the Robotics Institute, University of Michigan, Ann Arbor, MI, USA; galia@umich.edu

V. S. Chipade is with the Department of Aerospace Engineering, University of Michigan, Ann Arbor, MI, USA; vishnuc@umich.edu

D. Panagou is with the Department of Aerospace Engineering and with the Robotics Institute, University of Michigan, Ann Arbor, MI, USA; dpanagou@umich.edu

Manuscript 999 submitted to 2022 American Control Conference.
Received October 13, 2021.

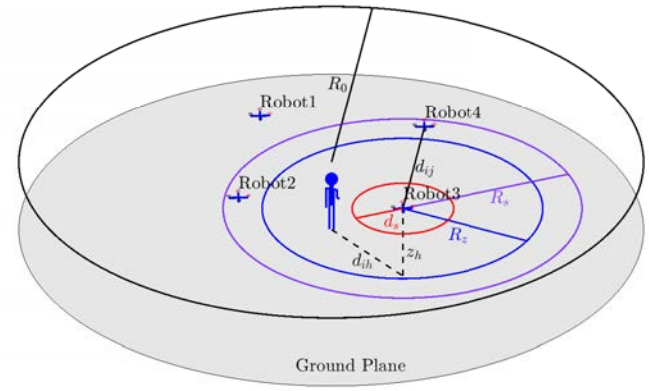

Fig. 1: Problem Setup

states. We then provide a robust leader-follower formation control based on the gradients of the Lyapunov-like functions from [9] that ensure the robots' convergence to a desired formation, their safety from each other and from the leader (human) and that the robots stay within a predefined area. Compared to the earlier work, the contributions of this paper are: 1) A gradient-based robust control law for leader-follower formation control that takes into account the uncertainties in the leader and followers' state measurements. 2) An experimental demonstration of the proposed robust control design using a team of quadrotor vehicles.

D. Organization

The rest of the paper is organized as follows. We describe the problem formulation in Section II. The leader-follower formation control algorithm without uncertainties and with uncertainties is described in Section III and IV, respectively. Simulations and experimental results are then provided in Section V and then finally the paper is concluded in Section VI.

II. Problem Formulation

Notation: The set of real numbers is denoted by $\mathbb{R}$ and the set of nonnegative real numbers is denoted by $\mathbb{R}_+$. A Euclidean norm is denoted by $||\bullet||$. The gradient of a scalar function V with respect to a vector $\boldsymbol{x}$ is denoted as $\nabla_{\boldsymbol{x}} V$.

We consider N robots indexed by $i \in I = \{1, ..., N\}$ operating in a 2D plane at an altitude of z_h above the ground (see Fig. 1). The robots have circular footprint of radius r_a and move under single integrator dynamics:

$$\dot{\boldsymbol{x}}_i = \boldsymbol{u}_i, \quad \boldsymbol{x}_i(0) = \boldsymbol{x}_{i0} \tag{1}$$

where $\boldsymbol{x}_i = [x_i,\ y_i]^T \in \mathbb{R}^2$ denotes the position of Robot i and $\boldsymbol{u}_i = [u_x,\ u_y]^T$ denotes the velocity input. A human is assumed to operate in a static circular zone of radius R_0 centered at (x_0, y_0) given by $\mathcal{W}_c = \{\boldsymbol{x} \in \mathbb{R}^2 | \|\boldsymbol{x} - \boldsymbol{x}_0\| < R_0\}$. The position and the velocity of the human is denoted by $\boldsymbol{x}_h = [x_h, y_h]^T$ and $\boldsymbol{v}_h = [v_{xh}, v_{yh}]^T$.

Each robot i has a local sensing zone of radius R_s around it defined by $Z_s = \{\boldsymbol{x} \in \mathbb{R}^2 | \|\boldsymbol{x} - \boldsymbol{x}_i\| < R_s\}$ and can access the information as stated in Assumption 1.

Assumption 1. *Each robot i measures i) its own position with an additive, zero mean, Gaussian noise $\boldsymbol{\epsilon} \sim \mathcal{N}(0, \Sigma_{\boldsymbol{\epsilon}})$ where covariance $\Sigma_{\boldsymbol{\epsilon}} = diag([\sigma_x^2, \sigma_y^2])$ is the covariance of the measurement noise, i.e., the measurement is $\bar{\boldsymbol{x}}_i = \boldsymbol{x}_i + \boldsymbol{\epsilon}$, ii) and the position and the velocity of the human with an additive uniformally distributed uncertainty Δ_p and Δ_v, respectively.*

Each robot exchanges the sensed information with other robots based on a connected undirected graph $G = (V, E)$. Each vertex of this graph corresponds to a robot so the set of vertices V is given by the indices of the robots, i.e, $V = \{1, 2, ..., N\}$, and an edge on this graph corresponds to a communication link between two robots so the set of edges E is given $E = \{(i, j) \in I \times I | \|\boldsymbol{x}_i - \boldsymbol{x}_j\| \leq R_s\}$. Here it is assumed that the robot i communicates information with other robot j whenever robot j is in the sensing zone of the robot i.

We also assume that the initial states of the robots are $\boldsymbol{x}_{i0} = \bar{\boldsymbol{x}}_i(0)$ for all $i \in I$. To ensure connected graph is formed, the robots are assumed to satisfy Assumption 2 as follow.

Assumption 2. *All robots and the human lie inside $\mathcal{W}_c$ at initial time $t = 0$ and are such that each robot has at least one other robot in its sensing zone so that a connected graph is formed.*

The goal of each robot i is to i) converge to a specified formation centered at the human, ii) remain completely within the connectivity region $\mathcal{W}_c$ so that a connected communication graph is maintained, and iii) avoid inter-robot and human-robot collisions by maintaining a safe distance $d_s > 2r_a$ from the other robots and human. Formally, the problem addressed in this paper is described as follows:

Problem 1. *Design a robust control action $\boldsymbol{u}_i$ for robot i for all $i \in I$, such that: i) the state $\boldsymbol{x}_i$ converges to a neighborhood of their goal location in the specified formation around the human, ii) robot i stays inside $\mathcal{W}_c$, i.e., $\|\boldsymbol{x}_i - \boldsymbol{x}_0\| < R_0 - r_a$, iii) robot i avoids collisions with other robots and the human, i.e. $\|\boldsymbol{x}_i(t) - \boldsymbol{x}_j(t)\| > d_s$ for all $j \neq i \in I$ and $\|\boldsymbol{x}_i(t) - \boldsymbol{x}_h(t)\| > d_s$ for all times $t > 0$, despite the noisy measurements as described in Assumption 1.*

III. Leader-Follower Formation Control

Before describing the solution to Problem 1, in this section, we briefly explain the Leader-Follower formation control with connectivity maintenance algorithm as designed in [9] for the case when the positions of the leader (human in this case) and the followers (the robots) are perfectly known.

Manuscript 999 submitted to 2022 American Control Conference.
Received October 13, 2021.

A. Connectivity Maintenance and Formation

Each robot i is to remain completely inside the circular region $\mathcal{W}_c$ at all times, i.e., $\|\boldsymbol{x}_i - \boldsymbol{x}_0\| < R_0 - r_a$. This can be equivalently written as the nonlinear inequality constraint:

$$c_{i0}(\boldsymbol{x}_i) = R - \|(\boldsymbol{x}_i - \boldsymbol{x}_0)\| \geq 0. \tag{2}$$

where $R = R_0 - r_a$. A logarithmic barrier function is defined $b_{i0}(\boldsymbol{x}_i) : \mathbb{R}^2 \to \mathbb{R}$ with the constraint

$$b_{i0}(\boldsymbol{x}_i) = -ln(c_{i0}(\boldsymbol{x}_i)) \tag{3}$$

which goes to $+\infty$ as $c_{i0}(\boldsymbol{x}_i) \to 0$. The gradient recentered barrier function can then be defined as:

$$r_{i0}(\boldsymbol{x}_i) = b_{i0}(\boldsymbol{x}_i) - b_{i0}(\boldsymbol{x}_{i,d}) - \nabla_{\boldsymbol{x}_i} b_{i0}|^T_{\boldsymbol{x}_{i,d}} (\boldsymbol{x}_i - \boldsymbol{x}_{i,d}) \tag{4}$$

where $\boldsymbol{x}_{i,d}$ is the location of the goal location. This leads to the gradient recentered barrier function for the constraint $c_{i0}(\boldsymbol{x}_i)$ where

$$\nabla_{\boldsymbol{x}_i} b_{i0}|_{\boldsymbol{x}_{i,d}} = \frac{1}{\|\boldsymbol{x}_{i,d} - \boldsymbol{x}_0\|(R - \|\boldsymbol{x}_{i,d} - \boldsymbol{x}_0\|)} (\boldsymbol{x}_{i,d} - \boldsymbol{x}_0) \tag{5}$$

where $\boldsymbol{x}_{i,d} = \begin{bmatrix} x_{i,d} & y_{i,d} \end{bmatrix}^T$ is the goal position of robot i, $\nabla_{\boldsymbol{x}_i} b_{i0} = \begin{bmatrix} \partial b_{i0}/\partial x_i & \partial b_{i0}/\partial y_i \end{bmatrix}^T$ is the gradient vector of the function $b_{i0}(\boldsymbol{x}_i)$, and $(\nabla_{\boldsymbol{x}_i} b_{i0}|_{\boldsymbol{x}_{i,d}})^T$ is the transpose of this gradient vector evaluated at the goal position $\boldsymbol{x}_{i,d}$. However, in this work the goal position $\boldsymbol{x}_{i,d}$ is redefined using leader-follower distance-based formation control and therefore can be redefined as

$$\boldsymbol{x}_{i,d} = \boldsymbol{x}_h + \mathbf{d}_i \tag{6}$$

where $\boldsymbol{x}_h$ is the position of the human, which is also acting as the leader in this case, and $\mathbf{d}_i \in \mathbb{R}^2$ is the fixed relative position that the robot i is to maintain around the human. With both connectivity maintenance and formation convergence considered, a Lyapunov-like function $V_{i0} : \mathbb{R}^2 \to \mathbb{R}^+$ is then defined as:

$$V_{i0}(\boldsymbol{x}_i) = (r_{i0}(\boldsymbol{x}_i))^2 \tag{7}$$

where V_{i0} is always a nonnegative function.

B. Collision Avoidance

The robots are also required to avoid collisions with other robots and the human. Let the distance between robot i and j be $d_{ij} = ||\boldsymbol{x}_i - \boldsymbol{x}_j||$. We want d_{ij} to be always greater than or equal to the safety distance d_s. That is equivalently written as:

$$c_{ij}(\boldsymbol{x}_i, \boldsymbol{x}_j) = (x_i - x_j)^2 + (y_i - y_j)^2 - d_s^2 \geq 0 \tag{8}$$

The logarithmic barrier function $b_{ij}(\boldsymbol{x}_i, \boldsymbol{x}_j) : \mathcal{R}_i \times \mathcal{R}_j \to \mathbb{R}$ is defined as

$$b_{ij}(\boldsymbol{x}_i, \boldsymbol{x}_j) = -ln(c(\boldsymbol{x}_i, \boldsymbol{x}_j)) \tag{9}$$

The barrier function $q_{ij} : \mathbb{R}^2 \times \mathbb{R}^2 \to \mathbb{R}$

$$q_{ij}(\boldsymbol{x}_i, \boldsymbol{x}_j) = b_{ij}(\boldsymbol{x}_i, \boldsymbol{x}_j) - b_{ij}(\boldsymbol{x}_{id}, \boldsymbol{x}_j) \tag{10}$$

which is 0 at the goal position $\boldsymbol{x}_{i,d}$ of robot i and tends to $+\infty$ as $c_{ij}(\boldsymbol{x}_i, \boldsymbol{x}_j) \to 0$, which occurs when the distance d_{ij} tends to the minimum separation distance d_s. To have an everywhere nonnegative function, we define the function $V_{ij}^{'} : \mathbb{R}^2 \times \mathbb{R}^2 \to \mathbb{R}^+$ as:

$$V'_{ij}(\boldsymbol{x}_i, \boldsymbol{x}_j) = q_{ij}(\boldsymbol{x}_i, \boldsymbol{x}_j)^2 \tag{11}$$

To activate the collision avoidance action corresponding to the robot j only when j is inside the sensing zone of robot i, a bump function is defined as follows:

$$\sigma_{ij} = \begin{cases} 1 & \text{if } d_s \leq d_{ij} \leq R_z \\ Ad_{ij}^3 + Bd_{ij}^2 + Cd_{ij} + D & \text{if } R_z < d_{ij} < R_s \\ 0 & \text{if } d_{ij} \geq R_s \end{cases}$$

where the coefficients are defined as $A = -(2/(R_z - R_s)^3)$, $B = (3(R_z + R_s)^3)$, $C = -(6R_zR_s/(R_z - R_s)^3)$, and $D = (R_s^2(3R_z - R_s)/(R_z - R_s)^3)$ so that σ_{ij} is a continuously differentiable function. Here $R_z < R_s$ is the radius inside which the collision avoidance is fully activated. The Lyaponuv-like function for collision avoidance between robots can then be defined as

$$V_{ij}(\boldsymbol{x}_i, \boldsymbol{x}_j) = \sigma_{ij} V'_{ij}(\boldsymbol{x}_i, \boldsymbol{x}_j) \tag{12}$$

here the bump function σ_{ij} allows a smooth transition from no collision avoidance action outside the sensing radius to a full collision avoidance action inside radius R_z. To combine the objectives of formation convergence and collision avoidance, the following Lyaponuv-like function is chosen

$$v_i(\boldsymbol{X}) = \left((V_{i0}(\boldsymbol{x}_i))^\delta + (V_{ih}(\boldsymbol{x}_i, \boldsymbol{x}_h))^\delta + \sum_{j \in I_i} (V_{ij}(\boldsymbol{x}_i, \boldsymbol{x}_j))^\delta \right)^{\frac{1}{\delta}} \tag{13}$$

where $\delta \in [1, +\infty)$, $I_i = \{j \in I | j \neq i\}$, $\boldsymbol{X} = [\boldsymbol{x}_1^T, \boldsymbol{x}_2^T, ..., \boldsymbol{x}_N^T, \boldsymbol{x}_h^T, R, d_s]^T$ is the collection of the positions of the robots and the human, and the hyperparameters R and d_s, and V_{ih} is the Lyapunov-like function similar to V_{ij} as in (12) with σ_{ih} as the corresponding bump function. The function $v_i : \mathbb{R}^{2(N+1)} \to \mathbb{R}^+$ is non-negative everywhere. The following function

$$V_i(\boldsymbol{X}) = \frac{v_i(\boldsymbol{X})}{1 + v_i(\boldsymbol{X})} \tag{14}$$

which is zero for $v_i = 0$, i.e., at the goal position $\boldsymbol{x}_{i,d}$ of the robot i, and is equal to 1 as $v_i \to \infty$. This Lyaponuv-like function is positive definite with respect to the goal formation position $\boldsymbol{x}_{i,d}$ (Theorem 1 in [9]).

C. Control Law

The control law for the robot i, using the gradient V_i can then be described as:

$$\boldsymbol{u}_i(t) = \boldsymbol{v}_h - \nabla_{\boldsymbol{x}_i} V_i|_{\boldsymbol{X}} \tag{15}$$

The following theorem proves the safety and the convergence of the robots' state trajectories to their desired formation.

Manuscript 999 submitted to 2022 American Control Conference.
Received October 13, 2021.

Theorem 1. *Under Assumption 2 and the control action* (15)*, each robot i converges to their goal location $\boldsymbol{x}_{i,d}$ around the human achieving the desired formation, stays within the connectivity region, i.e., $\|\boldsymbol{x}_i(t)-\boldsymbol{x}_0\| < R_0$, and avoids collision with other robots and the human, i.e., $\|\boldsymbol{x}_i(t)-\boldsymbol{x}_j(t)\| > d_s$ for all $j \neq i \in I$ and $\|\boldsymbol{x}_i(t)-\boldsymbol{x}_h(t)\| > d_s$ for all times $t > 0$.*

Proof: We have that $V_i(\boldsymbol{X}) = 0$ at $\boldsymbol{x}_i = \boldsymbol{x}_{i,d}$ and $V_i(\boldsymbol{X})$ is a positive definite function. In the absence of any possible collision conflicts between robot i and other robots and the human, i.e., when $\sigma_{ij} = 0$ for $j \neq i \in I$ and $\sigma_{ih} = 0$, the time derivative of $V_i(\boldsymbol{X})$ along the system trajectories is:

$$\begin{aligned}\dot{V}_i &= (\nabla_{\boldsymbol{x}_i} V_i|_{\boldsymbol{X}})^T \boldsymbol{u}_i + (\nabla_{\boldsymbol{x}_{i,d}} V_i|_{\boldsymbol{X}})^T \dot{\boldsymbol{x}}_{i,d} \\ &= (\nabla_{\boldsymbol{x}_i} V_i|_{\boldsymbol{X}})^T \boldsymbol{u}_i + (\nabla_{\boldsymbol{x}_{i,d}} V_i|_{\boldsymbol{X}})^T \boldsymbol{v}_h \\ &= (\nabla_{\boldsymbol{x}_i} V_i|_{\boldsymbol{X}})^T \boldsymbol{u}_i - (\nabla_{\boldsymbol{x}_i} V_i|_{\boldsymbol{X}})^T \boldsymbol{v}_h \\ &\qquad (\because \nabla_{\boldsymbol{x}_i} V_i = -\nabla_{\boldsymbol{x}_{i,d}} V_i) \\ &= -(\nabla_{\boldsymbol{x}_i} V_i|_{\boldsymbol{X}})^T \nabla_{\boldsymbol{x}_i} V_i|_{\boldsymbol{X}} < 0\end{aligned} \tag{16}$$

This implies $\dot{V}_i$ is negative definite and hence using Therem 4.1 in [14] we conclude that $\boldsymbol{x}_i$ converges to $\boldsymbol{x}_{id}$. As shown in [9] the gradient $\nabla_{\boldsymbol{x}_i} V_i$ becomes very large and points into the connectivity region at the boundary of $\mathcal{W}_c$ and away from the unsafe region around other robots and the human and hence each robot i stays inside the connectivity region $\mathcal{W}_c$ and avoids collision with other robots and the human.

IV. Robust Leader-Follower Formation Control

In this section, we discuss a robust control design based on (15), that accounts for the uncertainties in the measurements of the robots' state and human's state. We use the 'adaptive estimation by active-passive multi-agent system' algorithm [13] and a Kalman filter to estimate the human's state and the robot's own state, respectively. These estimation algorithms are discussed in the following subsections.

A. Adaptive Human State Estimation

In the adaptive active-passive multi-agent framework [13], the sensor state of the robot i is assumed to satisfy the following dynamics:

$$\dot{\xi}_i(t) = a\xi_i(t) + \eta_i(t) \tag{17}$$

where $\eta_i(t) \in \mathbb{R}$ is the control input and $a \in \mathbb{R},\ a \neq 0$. The sensor state ξ_i may contain the information from exogenous inputs, such as the position or velocity of the human, $c_h(t) \in \mathbb{R}, h = 1, ..., m, m \leq N$ sensed by each robot.

Each robot takes a measurement $\bar{\xi}_i$ of their sensor state corrupted with a time varying uncertainty, $\Delta_i(t) \in \mathbb{R}$ described by

$$\bar{\xi}_i(t) = \xi_i(t) + \Delta_i(t). \tag{18}$$

Then a distributed adaptive estimation algorithm as in [13] is given by:

$$\begin{aligned}\eta_i(t) = &-k_0\xi_i(t) - \alpha[\sum_{i\sim j}(\xi_i(t) - \xi_j(t) + \beta_i\xi_i(t))] \\ &+ p_i(t) - \alpha\sum_{i\sim h} k_{ih}(t)(\bar{\xi}_i(t) - c_h(t)) + v_i(t),\end{aligned} \tag{19}$$

$$\dot{p}_i(t) = -\gamma[\sum_{i\sim j}(\bar{\xi}_i(t) - \bar{\xi}_j(t) + \omega p_i(t)] + w_i(t), p_i(0) = 0, \tag{20}$$

where $p_i(t) \in \mathbb{R}$ denotes the integral action of robot i and $\alpha, \gamma, \omega \in \mathbb{R}_+$ are design parameters. $k_{ih}(t)$ is a smooth function that changes from 1 to 0 for the location of robot i and at the sensing radius of the robot i respectively and $\beta_i \in \bar{\mathbb{R}}_+$ is designed with at least one nonzero $\beta_i, i = 1, ..., N$. $v_i(t)$ and $w_i(t)$ are adaptive control signals for robot i with

$$\begin{aligned}v_i(t) \triangleq\ & k_0\hat{\Delta}_i(t) + \alpha[\textstyle\sum_{i\sim j}(\hat{\Delta}_i(t) - \hat{\Delta}_j(t)) + \beta_i\hat{\Delta}_i(t)] \\ &-\alpha\textstyle\sum_{i\sim h} k_{ih}(t)\hat{\Delta}_i(t),\end{aligned} \tag{21}$$

$$w_i(t) \triangleq \gamma[\sum_{i\sim j}(\hat{\Delta}_i(t) - \hat{\Delta}_j(t))] \tag{22}$$

where $\hat{\Delta}_i(t) \in \mathbb{R}$ is the estimation of the uncertainty. The update law can be described as

$$\dot{\hat{\Delta}}_i(t) = \Gamma\text{Proj}(\hat{\Delta}_i(t), -a(\tilde{\xi}_i(t) - \hat{\xi}_i(t) - \hat{\Delta}_i(t))), \tag{23}$$

with $\hat{\Delta}_i(0) = \hat{\Delta}_{i0}$ where $\Gamma \in \mathbb{R}_+$ is the adaptation rate and $\hat{\Delta}_{max} \in \mathbb{R}_+$ is the projection operator bound.

Theorem 2. *(Theorem 2 in [13]) For a given communication graph G, under the adaptive control signal given by 19 and 20 along with the corrective signals 21 and 22 and the update law 23, the closed-loop error of the N robot system satisfies:*

$$\|e_\xi(t)\| \leq \sqrt{\frac{\gamma_1}{\gamma_0}\kappa_1^2 + \frac{\Gamma^{-1}}{\gamma_0}\kappa_2^2} \tag{24}$$

where $e_\xi = [e_{\xi_1}, e_{\xi_2}, ..., e_{\xi_N}]^T$, $\gamma_0 \triangleq 0.5min(1, \gamma^{-1}), \gamma_1 \triangleq 0.5max(1, \gamma^{-1}, \kappa_1 \triangleq \frac{\alpha_2}{2\alpha_0} + (\frac{\alpha_2^2}{4\alpha_0^2} + \frac{2\Gamma^{-1}\alpha_2\eta_2}{\alpha_0})^{\frac{1}{2}}, \kappa_2 \triangleq \bar{\Delta} + \hat{\Delta}_{max}, \alpha_2 \triangleq \lambda_{min}(\mathcal{H}(G) + \mu I_N) \in \mathbb{R}_+, \alpha_0 \triangleq min(\alpha_1, \sigma) \in \mathbb{R}_+, \alpha_2 \triangleq \bar{\Delta}_d \in \mathbb{R}_+$.

The robots use the above adaptive active-passive algorithm to find an estimate $\hat{\boldsymbol{x}}_h = [\hat{x}_h, \hat{y}_h]^T$ of the position and $\hat{\boldsymbol{v}}_h = [\hat{v}_{xh}, \hat{v}_{yh}]^T$ of the velocity of the human by running the adaptive active-passive algorithm for each state x_h, y_h, v_{xh}, v_{yh}. Next, we describe the estimation of robot's own state from noisy measurements.

B. Robots' State Estimation

The state dynamics of the robot i and the measurement equation corresponding to its own state as per Assumption 1, are given as:

$$\begin{aligned}&\dot{\boldsymbol{x}}_i = \boldsymbol{u}_i, \quad \boldsymbol{x}_i(0) = \boldsymbol{x}_{i0}; \\ &\tilde{\boldsymbol{x}}_i = \boldsymbol{x}_i + \boldsymbol{\epsilon}_p\end{aligned} \tag{25}$$

Manuscript 999 submitted to 2022 American Control Conference.
Received October 13, 2021.

where $\boldsymbol{\epsilon}_p \sim \mathcal{N}(0, \Sigma_{\boldsymbol{\epsilon}_p})$ is a Gaussian noise. We use the following Kalman filter to find an estimate $\hat{\boldsymbol{x}}_i$ of the robot i's state using the measurement $\bar{\boldsymbol{x}}_i$.

$$\begin{aligned} \dot{\hat{\boldsymbol{x}}}_i &= \boldsymbol{u}_i + K(\hat{\boldsymbol{x}}_i - \bar{\boldsymbol{x}}_i), \qquad \hat{\boldsymbol{x}}_i(0) = \bar{\boldsymbol{x}}_i(0) \\ \dot{\Sigma}_{\tilde{\boldsymbol{x}}} &= -\Sigma_{\tilde{\boldsymbol{x}}}\Sigma_{\boldsymbol{\epsilon}_p}^{-1}\Sigma_{\tilde{\boldsymbol{x}}}, \qquad \Sigma_{\tilde{x}}(0) = \Sigma_{\boldsymbol{\epsilon}_p} \\ K &= -\Sigma_{\tilde{\boldsymbol{x}}}\Sigma_{\boldsymbol{\epsilon}_p}^{-1} \end{aligned} \tag{26}$$

where $\Sigma_{\tilde{\boldsymbol{x}}_i}$ is the covariance of the estimation error $\tilde{\boldsymbol{x}}_i = \boldsymbol{x}_i - \hat{\boldsymbol{x}}_i$.

Lemma 3. *The estimate $\boldsymbol{x}_i$ satisfies: $||x_i(t) - \hat{x}_i(t)|| \leq 3\sigma_x$ and $||y_i(t) - \hat{y}_i(t)|| \leq 3\sigma_y$ with 99.73% probability for all $t > 0$.*

C. Robust Control Law

Now, using the estimates of the human's state and robots' states, we design the following robust control action for robot i:

$$\boldsymbol{u}_i = \hat{\boldsymbol{v}}_h - \nabla_{\boldsymbol{x}_i} V_i|_{\hat{\boldsymbol{X}}} \tag{27}$$

where $\hat{\boldsymbol{v}}_h$ an estimate of human's velocity and $\hat{\boldsymbol{X}} = [\hat{\boldsymbol{x}}_1^T, \hat{\boldsymbol{x}}_2^T, ..., \hat{\boldsymbol{x}}_N^T, \hat{\boldsymbol{x}}_h^T, R_{robust}, d_{s,robust}]^T$ is the collection of all the estimated positions of robots and the human, and the robust hyper-parameters R_{robust} and $d_{s,robust}$. To ensure that the robots stay safe from other robots and the human despite using the estimated states in the control law (27), we make the following assumption about the robust safety parameter $d_{s,robust}$.

Assumption 3. *The robust safety parameter $d_{s,robust}$ satisfies $d_{s,robust} \geq d_s + 2\rho_1$ where $\rho_1 = 3\sqrt{\sigma_x^2 + \sigma_y^2}$.*

Assumption 3 essentially enlarges the safety distance to account for the uncertainties in the robots' states. Similarly, to ensure that the robots stay within the connectivity region despite using the estimated states in the control law (27), we make the following assumption about the robust parameter R_{robust} used in the calculation of $\nabla_{\boldsymbol{x}_i} V_i|_{\hat{\boldsymbol{X}}}$.

Assumption 4. *The robust parameter R_{robust} in (2) is chosen to be $R_{robust} = R - \rho_1$*

In Theorem 4 as described below, we provide formal guarantees on the convergence and safety under the robust control law (27).

Theorem 4. *Under Assumptions 1-4 and the robust control (27), with 99.73% probability, (i) the trajectories of each robot i converge to a ball of radius ρ_{max} around their goal position, i.e., there exists $T > 0$ such that $\|\boldsymbol{x}_i(t) - \boldsymbol{x}_{i,d}(t)\| < \rho_{max}$ for all $t > T$, (ii) stays within the connectivity region, i.e., $\|\boldsymbol{x}_i(t) - \boldsymbol{x}_0\| < R_0$, and (iii) avoids collision with other robots and the human, i.e., $\|\boldsymbol{x}_i(t) - \boldsymbol{x}_j(t)\| > d_s$ for all $j \neq i \in I$ and $\|\boldsymbol{x}_i(t) - \boldsymbol{x}_h(t)\| > d_s$ for all times $t > 0$.*

Proof: (i) In the absence of any possible collision conflicts between robot i and other robots and the human, i.e., when $\sigma_{ij} = 0$ for $j \neq i \in I$ and $\sigma_{ih} = 0$, the time derivative of $V_i(\boldsymbol{X})$ along the system trajectories is:

$$\begin{aligned} \dot{V}_i &= (\nabla_{\boldsymbol{x}_i} V_i|_{\boldsymbol{X}})^T \boldsymbol{u}_i + (\nabla_{\boldsymbol{x}_{i,d}} V_i|_{\boldsymbol{X}})^T \dot{\boldsymbol{x}}_{i,d} \\ &\overset{(27)}{=} (\nabla_{\boldsymbol{x}_i} V_i|_{\boldsymbol{X}})^T (\hat{\boldsymbol{v}}_h - \nabla_{\boldsymbol{x}_i} V_i|_{\hat{\boldsymbol{X}}}) + (\nabla_{\boldsymbol{x}_{i,d}} V_i|_{\boldsymbol{X}})^T \boldsymbol{v}_h \\ &= -(\nabla_{\boldsymbol{x}_i} V_i|_{\boldsymbol{X}})^T (\nabla_{\boldsymbol{x}_i} V_i|_{\hat{\boldsymbol{X}}} - (\boldsymbol{v}_h - \hat{\boldsymbol{v}}_h)) \end{aligned} \tag{28}$$

Let the maximum error in the estimation of human's position, as obtained from Theorem 2, be denoted by $e_{\boldsymbol{x}}$, i.e., $\|\boldsymbol{x}_h - \hat{\boldsymbol{x}}_h\| \leq e_{\boldsymbol{x}}$. We know from Lemma 3 that $\|\boldsymbol{x}_i - \hat{\boldsymbol{x}}_i\| < \rho_1$ with 99.73% This gives us:

$$(\nabla_{\boldsymbol{x}_i} V_i|_{\boldsymbol{X}})^T \nabla_{\boldsymbol{x}_i} V_i|_{\hat{\boldsymbol{X}}} > 0 \text{ for } \|\boldsymbol{x}_i - \boldsymbol{x}_{i,d}\| > \rho_1 + e_{\boldsymbol{x}}, \tag{29}$$

because both gradients point in the same direction (in fact toward the ball $\|\boldsymbol{x}_i - \boldsymbol{x}_{i,d}\| = \rho_1 + e_{\boldsymbol{x}}$), and $\boldsymbol{x}_i$ and $\hat{\boldsymbol{x}}_i$ both lie on the same side of $\boldsymbol{x}_{i,d}$, i.e., $(\boldsymbol{x}_i - \boldsymbol{x}_{i,d})^T(\hat{\boldsymbol{x}}_i - \boldsymbol{x}_{id}) > 0$. Now let the maximum error in the estimation of the human's velocity be denoted $e_{\boldsymbol{v}}$ (as obtained from Theorem 2), i.e., $\|\boldsymbol{v}_h - \hat{\boldsymbol{v}}_h\| \leq e_{\boldsymbol{v}}$. Away from the boundary of the connectivity region and the safety region around other robots and the human, we can find some $\lambda \in (0, 1)$ so that $\lambda V_i(\boldsymbol{X}) < \|\nabla_{\boldsymbol{x}_i} V_i|_{\boldsymbol{X}}\|$ [9]. This implies that we can find $\rho_2 > 0$ such that:

$$\min_{\|\boldsymbol{x}_i - \boldsymbol{x}_{i,d}\| = \rho_2} V_i = \frac{e_{\boldsymbol{v}}}{\lambda}. \tag{30}$$

This further implies:

$$e_{\boldsymbol{v}} < \|\nabla_{\boldsymbol{x}_i} V_i|_{\boldsymbol{X}}\| \quad \text{for } \|\boldsymbol{x}_i - \boldsymbol{x}_{i,d}\| > \rho_2 \tag{31}$$

Combining (29), (31) we have that:

$$\dot{V}_i < 0 \quad \text{for } \|\boldsymbol{x}_i - \boldsymbol{x}_{i,d}\| > \rho_{max} = \max(\rho_1 + e_{\boldsymbol{x}}, \rho_2) \tag{32}$$

Then using Theorem 4.18 in [14], we conclude that there exist some time $T > 0$ such that the trajectory of robot i converges within a ball of radius ρ_{max} around its goal position $\boldsymbol{x}_{i,d}$, i.e., $\|\boldsymbol{x}_i(t) - \boldsymbol{x}_{i,d}(t)\| < \rho_{max}$ for all $t > T$.

(ii) As proved in [9], the gradient $\nabla_{\boldsymbol{x}_i} V_i|_{\hat{\boldsymbol{X}}}$ becomes very large close to the boundary of $\mathcal{W}_c$ and points into the interior of $\mathcal{W}_c$ when $c_{i0}(\hat{\boldsymbol{x}}_i)$ becomes 0, that is when $\|\hat{\boldsymbol{x}}_i - \boldsymbol{x}_0\| = R_{robust}$. At this point, the maximum distance of the robot i's true position $\boldsymbol{x}_i$ from the center $\boldsymbol{x}_0$ is $\|\boldsymbol{x}_i - \boldsymbol{x}_0\|_{max} = \|\hat{\boldsymbol{x}}_i - \boldsymbol{x}_0\| + \rho_1$, with 99.73% probability. Now from Assumption 4 we have that $\|\boldsymbol{x}_i - \boldsymbol{x}_0\|_{max} = R_{robust} + \rho_1 = R = R_0 - r_a$ and hence the robot i stays inside $\mathcal{W}_c$.

(iii) The gradient $\nabla_{\boldsymbol{x}_i} V_i|_{\hat{\boldsymbol{X}}}$ also becomes very large near other robot j and points away from robot j when $c_{ij}(\hat{\boldsymbol{x}}_i, \hat{\boldsymbol{x}}_i)$ becomes 0, that is when $\|\hat{\boldsymbol{x}}_i - \hat{\boldsymbol{x}}_j\| = d_{s,robust}$. At this point the minimum distance between robot i and robot j is $\|\boldsymbol{x}_i - \boldsymbol{x}_j\|_{min} = \|\hat{\boldsymbol{x}}_i - \hat{\boldsymbol{x}}_j\| - \rho_1 - \rho_1$ with 99.73% probability. Now using Assumption 3 we get $\|\boldsymbol{x}_i - \boldsymbol{x}_j\|_{min} = d_{s,robust} - 2\rho_1 \geq d_s$ and hence robot i and robot j do not collide for any $i \in I$ and $j \in I$. Using similar arguments, one can establish that robot i also stays safe from the human under the robust control (27).

Manuscript 999 submitted to 2022 American Control Conference.
Received October 13, 2021.

V. Results

A. Simulations

In this section, we provide simulation results for a leader-follower formation control problem while considering uncertainty in sensing the leader and in the robot's own state estimation for validation of the proposed algorithm. We consider 4 robots that start at initial positions shown by blue stars in Fig. 5(a) that are connected based on a connected, undirected graph. A human leader visits 3 task locations marked by diamonds in Fig. 5(c). The parameters used in the simulation are given by $r_a = 1, R_0 = 30, \boldsymbol{x}_0 = [0.1, 0.1]^T, \sigma_x^2 = \sigma_y^2 = 0.1, R_s = 6, R_z = 3, \delta = 3, \boldsymbol{d}_1 = [0, 3]^T, \boldsymbol{d}_2 = [-3, 0]^T, \boldsymbol{d}_3 = [0, -3]^T, \boldsymbol{d}_4 = [3, 0]^T$ and parameters for the human state estimation are $a = 1, k_0 = 1, \gamma_x = \gamma_y = 20, \gamma_z = 30, \omega_x = \omega_y = 0.0045, \omega_v = 0.0033, \alpha_x = \alpha_y = 20, \alpha_v = 30, \beta = 0.001, i = 1, ..., 4, \mu = 1.5, \Gamma_x = \Gamma_y = 5, \Gamma_v = 8$, and $\Delta_p \in [0, 5]$ $\Delta_v \in [0, 1]$.

Figures. 5(a), Fig. 5(b), Fig. 5 (c), show the snapshots of the robots' and human's trajectories from the beginning until the human visits task 1, task 2 and task, respectively. As one can observe in this figures, the robots states converge close to their desired states in the formation around the human, which is also evident from Fig. 5(d) which shows the distances of the robots from their desired states. To assess the safety of the robots we plot the critical safety distances defined for each robot i as $\max_{j \neq i} \frac{d_{s,robust}}{d_{ij}}$ in Fig. 3. These critical safety distances have to be less than 1 for safety and as observed in Fig. 3 they are indeed less than 1 for all robots meaning the robots avoid both inter-robot and robot-human collisions. A simulation video can be found at https://tinyurl.com/estetatc

B. Experiments

We also demonstrated the proposed algorithm experimentally by deploying 4 quadrotor vehicles in the outdoor netted flying facility M-Air at the University of Michigan. Each quadrotor is equipped with a PixHawk orange cube autopilot board and a raspberry pi 4 computer for autonomous control and a Real-Time Kinetic (RTK) HERE3 GPS module for position measurements. A base RTK GPS module is connected to a ground station computer and sends the GPS corrections to each quadrotor (see Fig. 4). The raspberry pi and the ground station computer are connected on same wifi network and use Robot Operating System (ROS) to communicate messages. The pixhawk flight controller board communicates with the Raspberry pi using MAVROS, a ROS package, that uses MAVLink communication protocol, a special communication protocol designed for micro aerial vehicles.

The 4 quadrotors estimate the position of the state of the human. For safety reasons, the human trajectory is represented through a predefined trajectory. The same parameters used in the simulation section were used in the experiments, except the formation distances were increased to $\boldsymbol{d}_1 = [0, 4]^T, \boldsymbol{d}_2 = [0, -4]^T, \boldsymbol{d}_3 = [4, 0]^T, \boldsymbol{d}_4 = [-4, 0]^T$. The human had 1 task location marked with a box, at which point the human turned. The trajectory is shown in Figure. 5a, Fig. 5b, and Fig. 5c. The distances from the quadrotors' actual state to their goal locations are plotted in Fig. 7, which show that the trajectories of the quadrotors converge close to their desired trajectories with bounded error. Similar to the simulation results, critical safety distances are plotted in Fig. 8, which shows that the critical safety distances stay below 1 and therefore do indeed avoid inter-robot and robot-human collisions. We also performed an experiment with ground rover representing the human's motion. The videos of these both experiments can be found at: https://tinyurl.com/estetatc

VI. Conclusion

In this paper, we presented a robust leader-follower formation control algorithm using gradients of Lyapunov-like functions for the scenarios when the robots have noisy measurements of their own state as well as of the leader. A formation control for a team robots around a human that act as leader is studied using the proposed robust algorithm. The algorithm is tested in simulation as well as in experiments using a team of quadrotors. Future work can include considering higher order systems, considering obstacle avoidance in the environment, and using estimation of the human via vision algorithms.

VII. Acknowledgements

We thank our lab members Qilang Ding and Devansh Agrawal for their help during the experiments.

References

[1] H. T. Do, H. T. Hua, M. T. Nguyen, C. V. Nguyen, H. T. Nguyen, H. T. Nguyen, and N. T. Nguyen, "Formation control algorithms for multiple-uavs: A comprehensive survey," 2021.

[2] V. Roldão, R. Cunha, D. Cabecinhas, C. Silvestre, and P. Oliveira, "A leader-following trajectory generator with application to quadrotor formation flight," *Robotics and Autonomous Systems*, vol. 62, no. 10, pp. 1597–1609, 2014.

[3] Y. Zhao, L. Jiao, R. Zhou, and J. Zhang, "Uav formation control with obstacle avoidance using improved artificial potential fields," in *2017 36th Chinese Control Conference (CCC)*. IEEE, 2017, pp. 6219–6224.

[4] X. Dong, B. Yu, Z. Shi, and Y. Zhong, "Time-varying formation control for unmanned aerial vehicles: Theories and applications," *IEEE Transactions on Control Systems Technology*, vol. 23, no. 1, pp. 340–348, 2014.

[5] T. Dierks and S. Jagannathan, "Neural network control of quadrotor uav formations," in *2009 American Control Conference*. IEEE, 2009, pp. 2990–2996.

[6] Y. Liu and Y. Jia, "Adaptive leader-following consensus control of multi-agent systems using model reference adaptive control approach," *IET Control Theory & Applications*, vol. 6, no. 13, pp. 2002–2008, 2012.

[7] Y.-Y. Qian, L. Liu, and G. Feng, "Distributed event-triggered adaptive control for consensus of linear multi-agent systems with external disturbances," *IEEE transactions on cybernetics*, vol. 50, no. 5, pp. 2197–2208, 2018.

[8] Y. Su, P. Shi, X. Wang, and D. Xu, "Leader-following rendezvous for single-integrator multi-agent systems with uncertain leader," in *2017 11th Asian Control Conference (ASCC)*. IEEE, 2017, pp. 162–167.

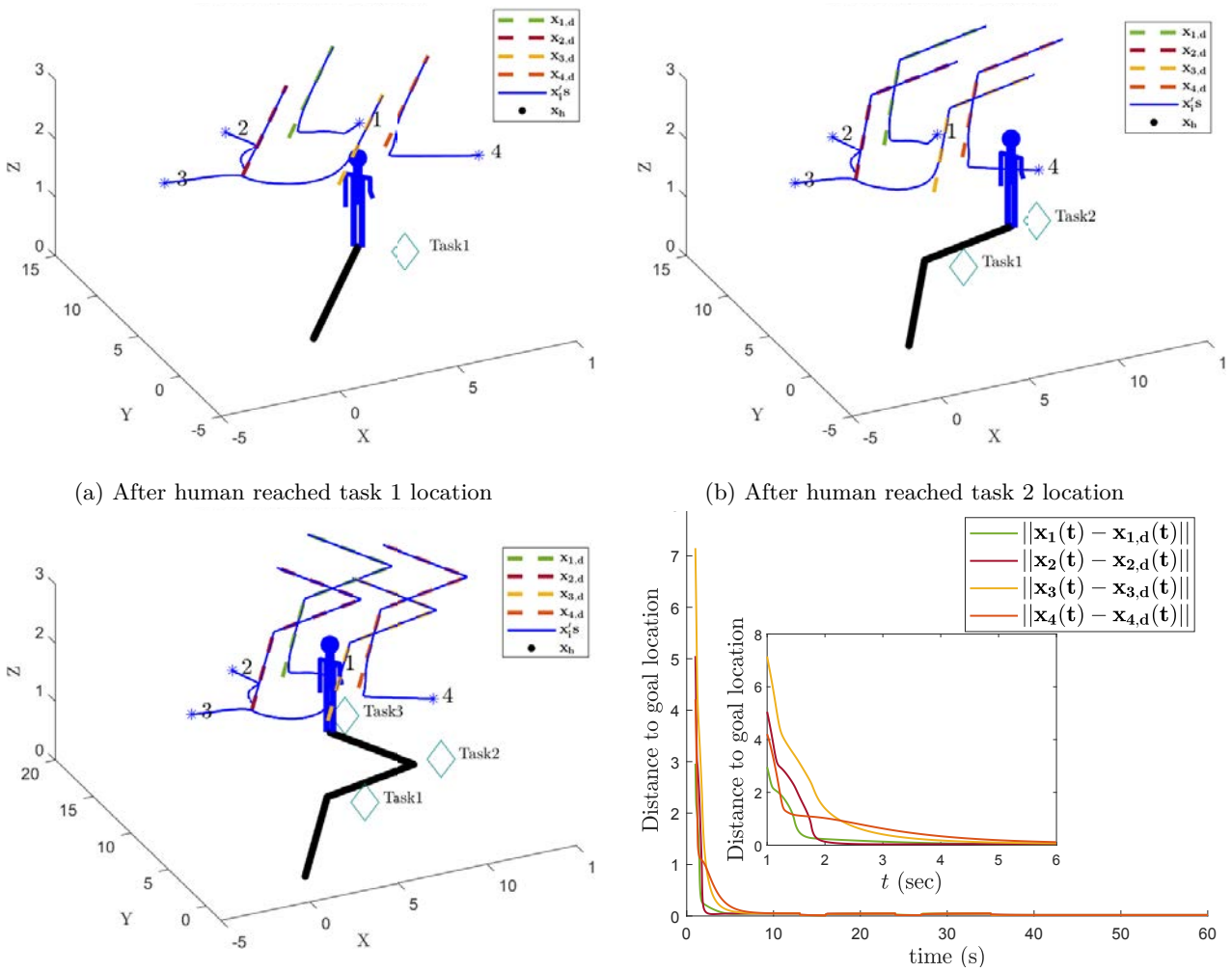

(a) After human reached task 1 location

(b) After human reached task 2 location

(c) After human reached task 3 location

(d) Convergence of actual state to their desired states

Fig. 2: Snapshots of robots' and human's trajectories and convergence of the actual states to their desired states

[9] D. Panagou, D. M. Stipanović, and P. G. Voulgaris, "Distributed coordination control for multi-robot networks using lyapunov-like barrier functions," *IEEE Transactions on Automatic Control*, vol. 61, no. 3, pp. 617–632, 2015.

[10] A. Filotheou, A. Nikou, and D. V. Dimarogonas, "Decentralized control of uncertain multi-agent systems with connectivity maintenance and collision avoidance," in *2018 European Control Conference (ECC)*. IEEE, 2018, pp. 8–13.

[11] D. Srivastava, D. M. Lofaro, T. Schuler, D. Sofge, and D. W. Aha, "Case-based gesture interface for multiagent formation control," in *International Conference on Case-Based Reasoning*. Springer, 2020, pp. 295–306.

[12] A. Suresh and S. Martínez, "Human-swarm interactions for formation control using interpreters," *International Journal of Control, Automation and Systems*, vol. 18, no. 8, pp. 2131–2144, 2020.

[13] E. Arabi, D. Panagou, and T. Yucelen, "Adaptive active-passive networked multiagent systems," in *2021 American Control Conference (ACC)*. IEEE, 2021, pp. 1113–1118.

[14] H. K. Khalil, *Nonlinear control*. Pearson New York, 2015.

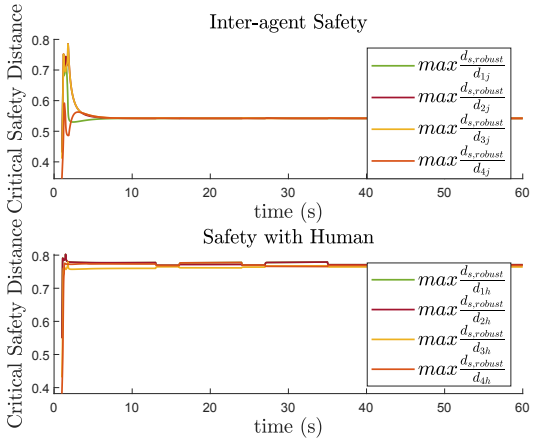

Fig. 3: Critical distances to assess safety

Manuscript 999 submitted to 2022 American Control Conference.
Received October 13, 2021.

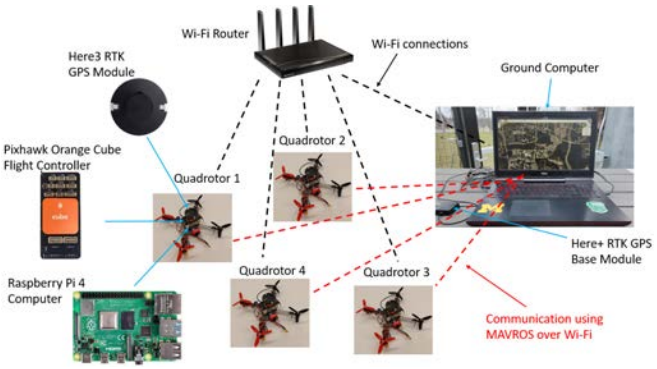

Fig. 4: Experimental Setup

(a) Human and the quadrotors at t=0

(b) After human reached task 1 location

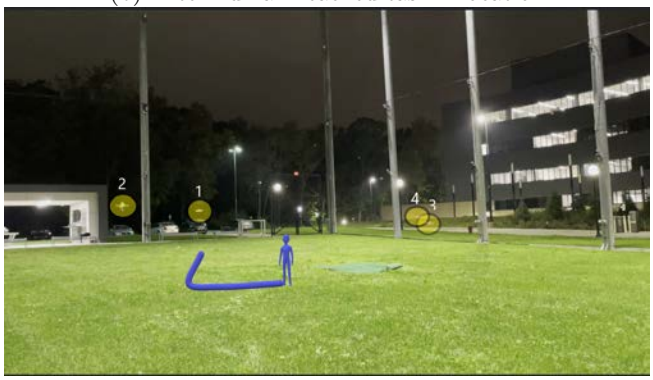

(c) After human reached task 2 location

Fig. 5: Snapshots of the configurations of quadrotors around the human during the experiment

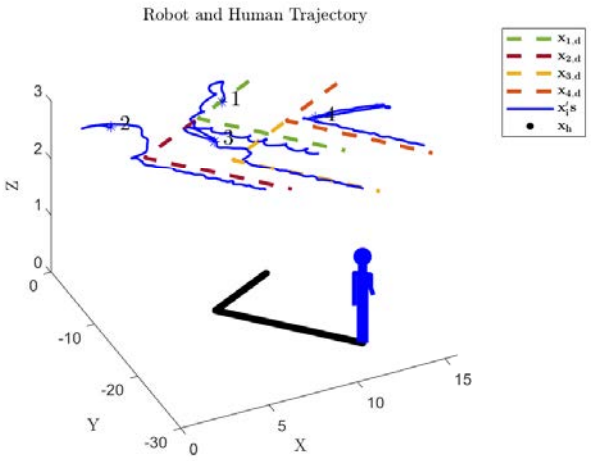

Fig. 6: The trajectories of the quadrotors and the human

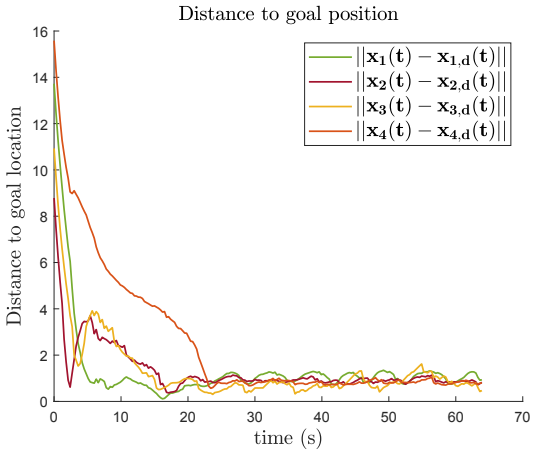

Fig. 7: Convergence of actual state to their desired states in experiments

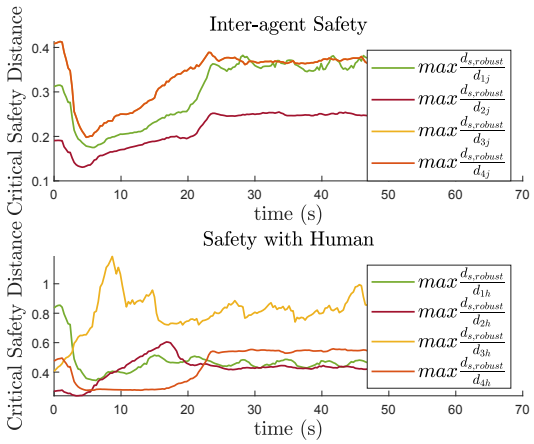

Fig. 8: Critical distances to assess safety in experiments

Manuscript 999 submitted to 2022 American Control Conference.
Received October 13, 2021.